ACS Sustainable Chemistry & Engineering

Research Article

pubs.acs.org/journal/ascecg

Hierarchically Structured Porous Nitrogen-Doped Carbon for Highly Selective CO_2 Capture

Di Li,[§,†] Yanli Chen,[§,‡] Min Zheng,[†] Haifeng Zhao,[†] Yunfeng Zhao,[*,‡] and Zaicheng Sun[*,†]

[†]State Key Laboratory of Luminescence and Applications, Changchun Institute of Optics, Fine Mechanics and Physics, Chinese Academy of Sciences, 3888 East Nanhu Road, Changchun, Jilin 130033, P. R. China

[‡]Institute for New Energy Materials & Low-Carbon Technologies, School of Materials Science and Engineering, Tianjin University of Technology, Tianjin 300384, P. R. China

Supporting Information

ABSTRACT: Nitrogen-doping has proven to be an effective strategy for enhancing the CO_2 adsorption capacity of carbon-based adsorbents. However, it remains challenging to achieve a high doping level of nitrogen (N) and a significant porosity in a carbon material simultaneously. Here we report a facile method that enables the fabrication of ordered macroporous nitrogen-doped carbon with the content of N as high as 31.06 wt %. Specifically, we used poly(EGDMA-*co*-MAA) microspheres as a template to fabricate the structure which can strongly interact with melamine (the precursor of nitrogen-doped carbon framework), self-assemble into three-dimensionally ordered structure, and be easily removed afterward. Upon chemical activation, significant microporosity is generated in this material without degrading its ordered macroporous structure, giving rise to a hierarchically structured porous nitrogen-doped carbon in which a remarkable N content (14.45 wt %) is retained. This material exhibits a moderate CO_2 adsorption capacity (2.69 mmol g^{-1} at 25 °C and 3.82 mmol g^{-1} at 0 °C under 1 bar) and an extraordinarily high CO_2/N_2 selectivity (134), which is determined from the single-component adsorption isotherms based on the ideal adsorption solution theory (IAST) method. This value far exceeds the CO_2/N_2 selectivity of thus-far reported carbon-based adsorbents including various nitrogen-doped ones. We believe that such an unprecedented CO_2/N_2 selectivity is largely associated with the unusually high N content as well as the partially graphitic framework of this material.

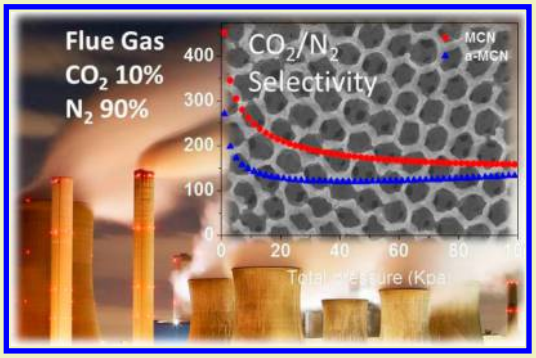

KEYWORDS: *Hierarchical porous nitrogen-doped carbon, Three-dimensional periodic structure, Nitrogen-doping, CO_2 capture, CO_2/N_2 selectivity*

INTRODUCTION

Nitrogen doping in carbon-based nanostructures has been an effective way to tailor the properties of carbon-based materials and render their potential applications in environmental issues including fuel cells, catalysis, photocatalysis, and CO_2 capture etc.[1−7] The nanoporous structures within the bulk of nitrogen-doped carbon have enhanced their performance in such applications due to not only the higher specific surface areas with larger number of active chemical sites but also porosities with efficient transport path and uniform pore size.[8−13] Therefore, synthesis of porous nitrogen-doped carbon materials using different approaches and precursors becomes a hot topic in the materials field.

CO_2 capture and sequestration (CCS) from the fuel exhaust of power plants is anxiously required due to the global warming issue.[14−16] According to the previous research in this field, hierarchically structured porous nitrogen-doped carbon is considered as ideal candidate for CO_2 capture due to its easy handling, abundant basic sites, size- and shape-selectivity and high surface area (micropores), easier mass-transfer to the adsorption sites (mesopores), and reduced pressure drop (macropores).[17−19] In addition to the adsorption capacity, the CO_2 selectivity, which is generally accepted to be related with the incorporation of nitrogen species, is of equal importance because practical applications are always associated with mixtures of different gases.[20−26] Until now, there are some meso/microporous nitrogen-doped carbons with different structures and controllable pore sizes constructed by the directing of hard and/or soft templates.[27,28] However, well-defined hierarchical porous nitrogen-doped carbons containing ordered macroporous skeletons have not been widely explored and reported due to the limited types of proper templates and the cumbersome procedures for construction. Therefore, facile synthesis of hierarchical porous nitrogen-doped carbons for effective CO_2 adsorption with high CO_2 selectivity is of important significance.

In this work, we report a facile procedure for synthesizing hierarchical macroporous nitrogen-doped carbons (MCN) with

Received: October 5, 2015
Revised: November 19, 2015
Published: November 23, 2015

DOI: 10.1021/acssuschemeng.5b01230
ACS Sustainable Chem. Eng. 2016, 4, 298−304

ordered three-dimensional periodic structures. We explore monodisperse polymer microspheres (EGDMA-*co*-MAA) which are rich in carboxyl groups on the surface as a template and melamine as the carbon and nitrogen source to construct the desired structures. In this system, carboxyl groups on the template can interact with melamine, which will fix the sources around the templates. With the following self-assembly of template and calcination, the hierarchical porous structures supported by periodic macroporous skeletons can be easily constructed during the formation process of graphitic nitrogen-doped carbon with simultaneous decomposition of the polymer templates. The resultant nitrogen-doped carbon materials possess relatively high nitrogen contents and large amounts of narrow micropores (<1 nm) can be generated in the bulk by KOH activation, which are all of benefit to CO_2 adsorption. The CO_2 adsorption performances of the materials are evaluated, and they exhibit considerable CO_2 adsorption capacity accompanied by inspiringly high CO_2-over-N_2 selectivity up to 158 and 134, respectively.

MATERIALS AND METHODS

Materials. All the chemicals were purchased from Sigma-Aldrich. Monodisperse microspheres of poly(EGDMA-*co*-MAA) were prepared by distillation precipitation copolymerizations of MAA (methacrylic acid) with EGDMA (ethylene glycol dimethacrylate) as cross-linking agent in neat acetonitrile and the diameter of the microspheres could be tuned successively in the range of hundred nanometers.[29]

Preparation of MCN. Melamine (150 mg) was first dissolved in H_2O (13 mL) at 100 °C, and poly(EGDMA-*co*-MAA) (100 mg) dispersion (in 2 mL H_2O) was subsequently added into the solution of melamine. The mixture was stirred for 16 h at 100 °C in a capped container and then centrifuged at 8000 rpm for 10 min after cooling down. The residual precursor was dried and transferred into a capped ceramic crucible, followed by heating to 600 °C with a rate of 2.5 °C min^{-1} under nitrogen in a furnace tube and kept at 600 °C for another 4 h to decompose polymer spheres and carbonize the precursor.

Chemical Activation. MCN was immersed into aqueous solution of KOH with the weight ratio of KOH/carbon = 2:1. The mixture was stirred and heated to evaporate the water. Then the drying product was heated under a N_2 atmosphere at a rate of 3 °C min^{-1} and kept at 600 °C for 1 h. The activated sample (a-MCN) was sequentially washed with diluted HCl and distilled water until the pH was neutral.

Characterization. Fourier transform infrared (FT-IR) spectra were recorded on a Bruker Vertex 70 spectrometer. Scanning electron microscope (SEM) images were measured on a JEOL JSM 4800F. Transmission electron microscope (TEM) images were taken using an FEI Tecnai G2 operated at 200 kV. For TEM observations, the samples were dispersed in ethanol and then dried on a lacey carbon film Cu grid. X-ray photoelectron spectra (XPS) were obtained on a Thermo Scientific ESCALAB 250 multitechnique surface analysis. The crystalline structure was recorded by using an X-ray diffractometer (XRD) (Bruker AXS D8 Focus), using Cu Ka radiation (λ = 1.54056 Å). The Brunauer–Emmett–Teller (BET)[30] specific surface area was measured using a Micromeritics ASAP 2020 sorption analyzer. Thermogravimetric analyses (TGA) were performed on a TA Q500 thermogravimeter in N_2 atmosphere. The contents of C, N, and H in nitrogen-doped carbon materials were determined using a Thermo Flash EA 1112 spectrometer.

Gas Adsorption Measurement. The CO_2 and N_2 adsorption isotherms at different temperatures (0 and 25 °C) were all collected on a Micromeritics ASAP 2020 sorption analyzer. The gas purity was 99.9999% for N_2 and 99.9995% for CO_2. Before the adsorption analysis, the sample was degassed at 300 °C for 10 h under vacuum. The measurements under different temperatures and gases were taken consecutively without redegassing. The temperatures were controlled by means of a circulating bath.

The Breakthrough Measurement. MCN or a-MCN (650 mg) powder was fully grounded and packed in a quartz column (5.8 mm I.D. × 150 mm) with quartz wool filling the void space. The sample was in situ activated under He flow (5 mL min^{-1}) at 200 °C for 24 h to remove adsorbed molecules and make the active sites accessible. The sample was then continuously purged with He flow (5.0 mL min^{-1}) for 1 h, while the temperature of the column was decreased to room temperature (25 °C). The mix gas (CO_2:N_2 = 1:9 by volume) flow was then introduced at 5.0 mL min^{-1}. Effluent from the column was monitored using a mass spectrometer.

RESULTS AND DISCUSSION

The typical preparation procedure of periodic macroporous nitrogen-doped carbon is shown in Figure 1. Polymer spheres

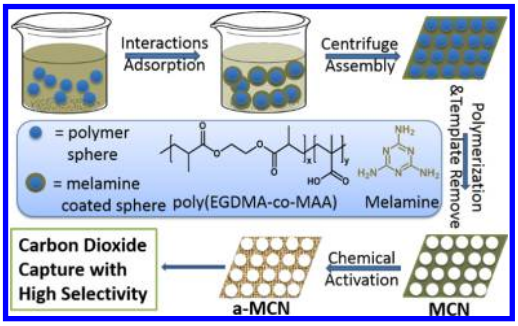

Figure 1. Synthesis process of materials and illustration chemical structures of polymer and melamine.

(poly(EGDMA-*co*-MAA)) were used as template to construct periodic structure and stirred with melamine in boiled water. During the centrifugation process, well-defined melamine coated polymer spheres (precursor) were packed up through a self-assembly process (Supporting Information, Figure S1).[31] The precursor transformed into nitrogen-doped carbon after heating at 600 °C for 4 h (25% yield). Notably, the organic templates were removed accompanying with the carbonization of precursor. On the contrary, the removal process of silica spheres hard template involves ammoniumbifluo (NH_4HF_2) or hydrogen fluoride (HF), which is hazardous and not environmentally friendly. As a result, the MCN was successfully prepared by using this greener and facile method.

As shown in the FTIR spectra (Figure 2), the carbonyl (C═O) stretching band at 1720 cm^{-1} in polymer template shifts and breaks into 1716 and 1683 cm^{-1} in precursor, which corresponds to H-bonding involvement of C═O with NH in

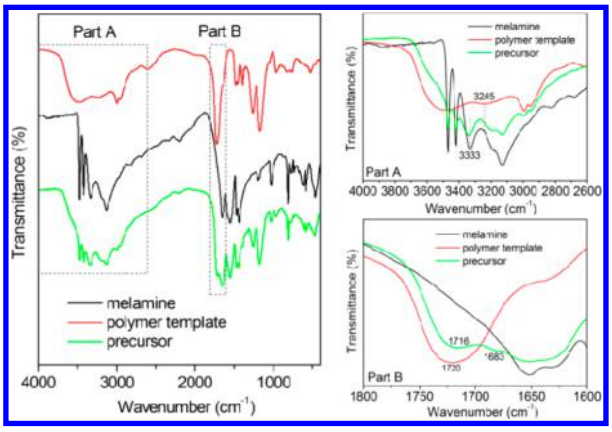

Figure 2. FTIR spectra of melamine, polymer template, and precursor.

DOI: 10.1021/acssuschemeng.5b01230
ACS Sustainable Chem. Eng. 2016, 4, 298–304

melamine.[32,33] There are strong intermolecular hydrogen bonds in the solids of melamine with H-bonded NH stretching band (ν NH) around 3333 cm^{-1}, and this ν NH broadens with a maximum at 3340 cm^{-1} in the precursor. During the solution processing, original hydrogen bonds (C═N···HN) in melamine break up and hydrogen bonds (C═O···HN) between melamine and the polymer form to a certain extent. After cooling down and centrifugation, both C═O···HN and reformed C═N···HN are presented in the precursor which contribute to the broadening thus the subtle shift of ν NH.[34] Because there is a majority of melamine besides the melamine/polymer assembly in the precursor, the variations of ν NH could not be obviously resolved in FTIR spectra by the influence of strong melamine signals. Moreover, ν OH at 3245 cm^{-1} in the polymer template shifts and contributes to the broad absorption band at 3199 cm^{-1} in the precursor, which indicated the possibility of intermolecular OH···N H-bonding.[33,35]

The TGA curves (Supporting Information, Figure S2) of the polymer, melamine, and precursor show that the polymer template can maintain its major mass below 400 °C, under which melamine has sublimated and formed polymeric melamine.[36] Accompanied by the decomposition of polymer sphere at high temperature, the fractional decomposed component of the polymer template also incorporated into the condensed melamine and thus constructed the ordered macroporous nitrogen-doped carbon. There is a platform of 8% residual mass upon 500 °C for precursor, which indicates the formation of thermostable nitrogen-doped carbon network.

Interestingly, both the precursor (Supporting Information, Figure S3) and product (MCN) exhibit characteristic structural colors (Figure 3a) which reflects the ordered arrangement of

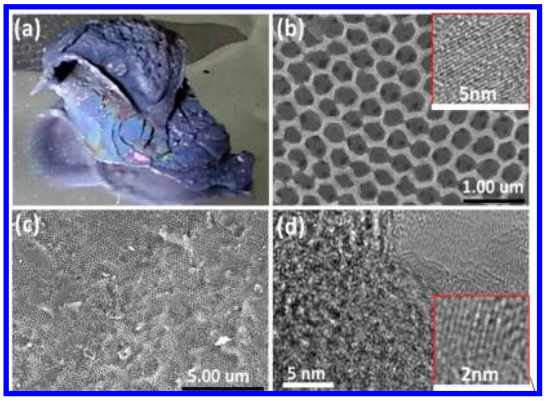

Figure 3. (a) Optical image of MCN. (b) SEM image of MCN. Inset: HRTEM crystallization stripes image of MCN. (c) SEM image of a-MCN. (d) HRTEM image and crystallization stripes (inset) of a-MCN.

colloidal crystal templates in precursor and the periodic structure in products. The formation of 3D periodic macroporous structure (we use polymer template whose diameter distributes in the range of 350−370 nm for example) is confirmed by scanning electron microscope (Figure 3b; Supporting Information, Figure S4). The macropore size estimated from SEM is around 350 nm, which illustrates that polymer spheres act as template. The 3D ordered macropores structure appears to be typical face-centered cubic (fcc), which can be observed in the (100) plane, with each pore surrounded by six equal pores in layers perpendicular to the (111) direction. A representative low-magnification transmission electron microscope image (Supporting Information, Figure S5) further demonstrates its ordered macropore arrays.

Chemical activation was performed on MCN with KOH at a mild temperature in order to construct hierarchical porous structures with increased specific surface area, especially the microporous surface areas. The continuous macroporous structure endowed efficient KOH impregnation and activation. The KOH activated MCN (denoted as a-MCN, 12% yield) still kept its original periodic 3D porous structure as confirmed by SEM (Figure 3c). Chemical reactions of KOH with the MCN bulk made a large amount of nanoscale pores generated in the final products that can be observed in high resolution transmission electron microscope (HRTEM) image (Figure 3d).

The powder X-ray diffraction (XRD) patterns (Figure 4a) of both MCN and a-MCN show two broad (002) reflections,

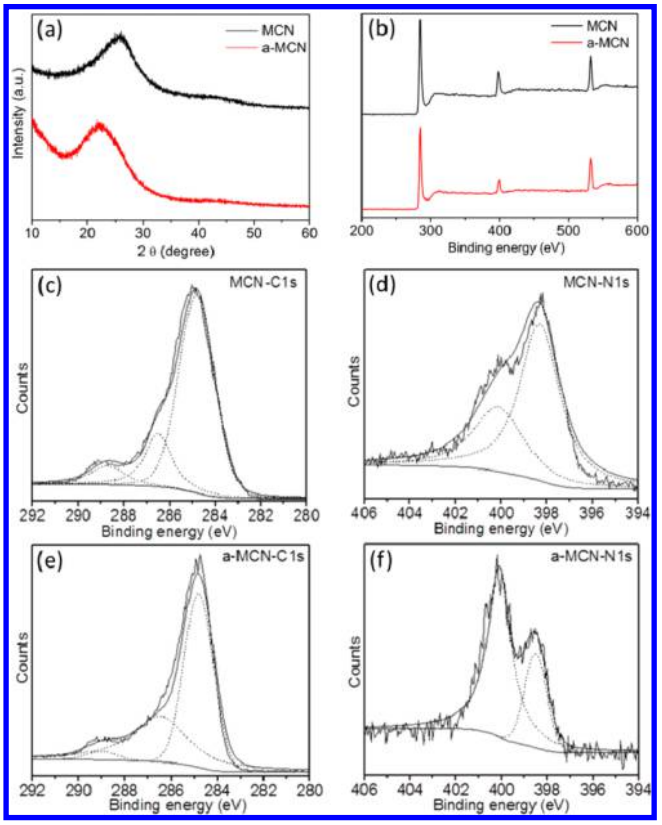

Figure 4. (a) XRD patterns, (b) XPS survey, C 1s (c) and N 1s (d) spectra of MCN and C 1s (e) and N 1s (f) a-MCN.

indicating that there is turbostratic ordering of carbon and nitrogen atoms in the MCN graphene layers, which is similar to that in bulk CN materials reported previously.[11,12] HRTEM images of the two materials exhibit certain crystallized domains at the wall of the skeletons (Supporting Information, Figure S6), which reveal certain graphitic nature of the two composites. The Raman spectrum of MCN (Supporting Information, Figure S7) shows two strong broad bands at 1364 and 1576 cm^{-1} that can be assigned to the D and G bands of the disordered and graphitized carbons, respectively.[5,9] The comparable intensity of D and G bands also suggests that MCN is partially composed of graphitic moieties. X-ray photoelectron spectroscopy (XPS) spectra (Figure 4b−f; Supporting Information, S8) confirm that MCN is composited of carbon,

DOI: 10.1021/acssuschemeng.5b01230
ACS Sustainable Chem. Eng. 2016, 4, 298−304

nitrogen, and some amounts of oxygen. In the deconvoluted C 1s spectrum, the major peak at 284.8 eV is assigned to C−C coordination and the weaker ones at 286.5 and 288.7 eV are identified as the sp^2 C atom bonded to N in an aromatic ring and C−O component, respectively. The N 1s spectrum of MCN is assigned to two binding energies including 398.3 eV for pyridine nitrogen and 400.2 eV for pyrrole nitrogen and/or graphitic nitrogen.[4,23,37−39] After KOH activation, the relative amount of nitrogen has decreased especially for the peak at 398.3 eV, suggesting that most of the lost nitrogen species during the activation process are associated with pyridine nitrogen.[20,23] Elemental analysis reveals that the nitrogen, carbon, and hydrogen contents are 31.06%, 60.35%, and 1.36% in MCN, while the relative values for a-MCN are 14.45%, 62.03%, and 1.93%, respectively. After activation, over half loss of nitrogen was found for a-MCN. The nitrogen content of MCN is far higher than reported nitrogen-doped porous carbons, and even after activation, the N content of a-MCN is still one of the highest N-contents among porous N-doped carbons.[20,23,40−46] The relatively high nitrogen contents of MCN and a-MCN reveal that they may act as excellent candidates for CO_2 capture with high selectivity under low pressure (<1 bar). Texture property is important to affect CO_2 capture performance of porous nitrogen-doped carbons. The N_2 adsorption isotherms of the two samples are shown in Figure 5a and reveal the hierarchical nanoporous structures of

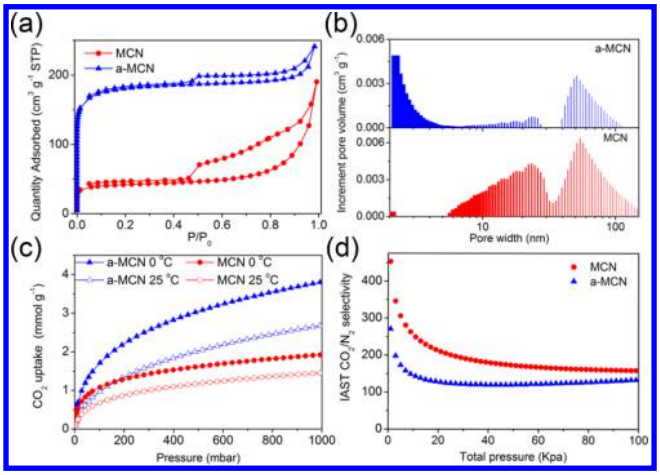

Figure 5. N_2 adsorption isotherms under −196 °C (a), pore distribution calculated by NLDFT method (b), CO_2 adsorption isotherms at 0 and 25 °C (c), and IAST selectivity curves under 25 °C (d) of MCN and a-MCN.

the two materials. The Brunauer−Emmett−Teller (BET)[30] surface area increased from 156 $m^2\ g^{-1}$ for MCN to 692.80 $m^2\ g^{-1}$ for a-MCN, and the relative micropore surface area increased from 118.04 to 594.75 $m^2\ g^{-1}$ after activation as summarized in Table 1. During the activation process, pores from 5 to 30 nm disappeared and around 2 nm were generated in a-MCN (Supporting Information, Figure 5b). Most importantly, a large amount of narrow micropores (<1 nm) are generated in a-MCN during chemical activation (Supporting Information, Figure S9), which is beneficial to CO_2 capture under low pressure (<1 bar).

On the basis of the nitrogen incorporated, interconnected porous characters of these materials, CO_2 adsorption has been performed on both MCN and a-MCN and adsorption isotherms at 0 and 25 °C are shown in Figure 5c. As given in Table 1, The MCN sample exhibited a CO_2 adsorption capacity of 1.46 mmol g^{-1} at 25 °C and 1.93 mmol g^{-1} at 0 °C under the ambient pressure, while the adsorption capacity of a-MCN increased to 2.69 mmol g^{-1} at 25 °C and 3.82 mmol g^{-1} at 0 °C. The increasing of CO_2 capacity after activation is ascribed to the generation of large amounts of narrow micropores.

To evaluate the CO_2 to N_2 selectivity which was as important as the capacity of sorbents for postcombustion application, nitrogen adsorptions on MCN and a-MCN were investigated under 0 and 25 °C (Supporting Information, Figure S10). Although MCN and a-MCN only displayed the moderate CO_2 capacity which was probably due to their low surface area, the two samples exhibited more preferential adsorption of CO_2 over N_2. Ideal adsorption solution theory (IAST)[47] was used to evaluate CO_2-over-N_2 selectivity based on the single-component gas adsorption results. The accuracy of the IAST procedure has already been established for adsorption of a wide variety of gas mixtures in many porous materials.[48−50] As shown in Figure 5d, both the samples exhibit remarkable CO_2/N_2 adsorption selectivity of 158 for MCN and 134 for a-MCN at 25 °C under CO_2 concentration of 10% (partial pressure of 0.1 bar) under total pressure of 100 KPa, which are exceptionally high in the reported hetero atoms-doped (ca. N, S) carbon porous materials (whose selectivity is listed in Supporting Information, Table S1, and less than 50 normally).[5,21,23,24]

To examine the real separation ability, the breakthrough experiments of separation flue gas were performed on both of MCN and a-MCN, in which a CO_2/N_2 (1:9, v/v) mixture was flowed over a packed bed of MCN or a-MCN solid with a total flow of 5 mL min^{-1} at 25 °C, respectively. The breakthrough curves are shown in Figure 6, and the separation of CO_2/N_2 mixture through the column packed bed of MCN or a-MCN solid can be efficiently achieved. For MCN, N_2 appeared downstream shortly after (45 s) the gas mixture being introduced into the column, while CO_2 was not detected until a breakthrough time of 1086 s. The adsorption capacities for N_2 and CO_2 were calculated to be 0.09 and 2.36 wt %, respectively, corresponding to a high CO_2/N_2 selectivity of 145. Although larger CO_2 capacity (3.58 wt %) was obtained from a-

Table 1. Textural Properties, CO_2 Adsorption Capacity, and the Breakthrough Results of MCN and a-MCN

materials	BET surface area (m^2/g)	micropore surface area (m^2/g)	N content (wt %)	CO_2 adsorption capacity (mmol g^{-1}) 273 K	298 K	IAST selectivity CO_2/N_2 (1/9), 298 K	breakthrough selectivity CO_2/N_2 (1/9), 298 K
MCN	156	118.04	31.06	1.93	1.46	158	145
a-MCN	682.80	594.75	14.45	3.82	2.69	134	70

DOI: 10.1021/acssuschemeng.5b01230
ACS Sustainable Chem. Eng. 2016, 4, 298−304

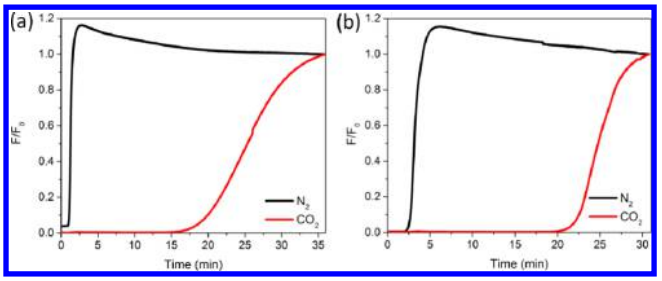

Figure 6. Breakthrough curves of (a) MCN and (b) a-MCN.

MCN (Figure 6b), the longer N_2 breakthrough time (114 s, 0.31 wt %) was recorded as well. Therefore, the CO_2/N_2 selective factor of 70 was obtained from a-MCN, which was less than that of MCN. MCN gives a better selectivity than a-MCN for both IAST and breakthrough experiment (Table 1). The CO_2 isosteric heats of adsorption (Q_{st}) (Supporting Information, Figure S11) on the two samples are calculated from the adsorption isotherms at 0 and 25 °C by using Clausius−Clapeyron relation, which can further prove the chemical affinity of porous sorbents to CO_2. The Q_{st} values at the initial adsorption stage (low gas loading) are 41.6 kJ mol^{-1} for MCN and 38.8 kJ mol^{-1} for a-MCN. They are much higher than the Q_{st} of activated carbon (~20 kJ mol^{-1}) and similar to values for some other amine-functionalized materials.[14,17] MCN has higher Q_{st} under low coverage range compared with the activated counterpart a-MCN, which reflects the higher interaction strength between MCN and CO_2. The probable reason is that MCN contains more nitrogen moieties which may act as active sites to adsorb CO_2 by polar interactions.[26] It should be pointed out that both MCN and a-MCN contained partial graphitic nano domains (Figure 3b and Figure 3d and Supporting Information, Figure S6), which could also help materials to enhance the CO_2 adsorption and therefore the selectivity to N_2 by introducing defects and curved regions.[30] As mentioned above, activation by KOH has consumed certain nitrogen moieties within the sample and generated a lot of micropores. It is widely investigated and accepted that porous materials with a large amount of micropores rather than mesopores and macropores would favor the CO_2 equilibrium adsorption.[26] However, larger pores (ca. macropores) would also benefit CO_2 capturing and separation once the porous materials are applied to resolve the difficulties in the industrial processes such as reducing the pressure drop over the materials and enhancing the CO_2 capacity from low concentration flue gas.[51,52]

CONCLUSION

In summary, we have explored a facile approach to construct three-dimensional macroporous nitrogen-doped carbon with periodic ordered macropores and further etched micropores on the skeletons by KOH activation. These hierarchical porous nitrogen-doped carbons are partly graphitic and possess relatively high nitrogen contents. Activation has increased the specific surface area of the MCN obviously due to the generation of micropores around 2 nm and narrow micropores (<1 nm), which endows this sample with moderate CO_2 adsorption capacity (2.69 mmol g^{-1} at 25 °C and 3.82 mmol g^{-1} at 0 °C under 1 bar). Notably, this kind of nitrogen-doped carbon exhibits excellent CO_2/N_2 selectivity up to 134 and it makes this kind of hierarchical porous nitrogen-doped carbons promising candidates for industrially CO_2 capture and sequestration.

ASSOCIATED CONTENT

Supporting Information

The Supporting Information is available free of charge on the ACS Publications website at DOI: 10.1021/acssuschemeng.5b01230.

CO_2/N_2 selectivity calculation by IAST, details of the breakthrough experiments, additional characterizations of MCN/a-MCN by optical, SEM, and TEM images, TGA curves, Raman and XPS spectra, micropore size distributions and N_2 adsorption−desorption isotherms (PDF)

AUTHOR INFORMATION

Corresponding Authors

*For Z.S.: E-mail, sunzc@ciomp.ac.cn.
*For Y.Z.: E-mail, yfzhao@tjut.edu.cn.

Author Contributions

§Di Li and Yanli Chen contributed equally.

Notes

The authors declare no competing financial interest.

ACKNOWLEDGMENTS

This work was supported by the National Natural Science Foundation of China (61306081, 61176016, 21402136), Natural Science Foundation of Jilin Province (20130522142JH), China Postdoctoral Science Foundation (2013M541716), Scientific Research Foundation for the Returned Overseas Chinese Scholars (K510900314), and the Specialized Research Fund for the Doctoral Program of Higher Education of China (20133201120004).

REFERENCES

(1) Wei, W.; Liang, H.; Parvez, K.; Zhuang, X.; Feng, X.; Müllen, K. Nitrogen-doped carbon nanosheets with size-defined mesopores as highly efficient metal-free catalyst for the oxygen reduction reaction. *Angew. Chem., Int. Ed.* **2014**, *53* (6), 1570−1574.
(2) Wang, Y.; Wang, X.; Antonietti, M. Polymeric graphitic carbon nitride as a heterogeneous organocatalyst: from photochemistry to multipurpose catalysis to sustainable chemistry. *Angew. Chem., Int. Ed.* **2012**, *51* (1), 68−89.
(3) Wang, X.; Maeda, K.; Chen, X.; Takanabe, K.; Domen, K.; Hou, Y.; Fu, X.; Antonietti, M. Polymer semiconductors for artificial photosynthesis: hydrogen evolution by mesoporous graphitic carbon nitride with visible light. *J. Am. Chem. Soc.* **2009**, *131* (5), 1680−1681.
(4) Liang, J.; Zheng, Y.; Chen, J.; Liu, J.; Hulicova-Jurcakova, D.; Jaroniec, M.; Qiao, S. Z. Facile oxygen reduction on a three-dimensionally ordered macroporous graphitic C_3N_4/carbon composite electrocatalyst. *Angew. Chem., Int. Ed.* **2012**, *51* (16), 3892−3896.
(5) Feng, S.; Li, W.; Shi, Q.; Li, Y.; Chen, J.; Ling, Y.; Asiri, A. M.; Zhao, D. Synthesis of nitrogen-doped hollow carbon nanospheres for CO_2 capture. *Chem. Commun.* **2014**, *50* (3), 329−331.
(6) Shi, Q.; Zhang, R.; Lv, Y.; Deng, Y.; Elzatahrya, A.; Zhao, D. Y. Nitrogen-doped ordered mesoporous carbons based on cyanamide as the dopant for supercapacitor. *Carbon* **2015**, *84*, 335−346.
(7) Shen, W.; Fan, W. Nitrogen-containing porous carbons: synthesis and application. *J. Mater. Chem. A* **2013**, *1* (4), 999−1013.
(8) Xia, Y.; Yang, Z.; Mokaya, R. Mesostructured hollow spheres of graphitic N-doped carbon nanocast from spherical mesoporous silica. *J. Phys. Chem. B* **2004**, *108* (50), 19293−19298.

(9) Liang, J.; Du, X.; Gibson, C.; Du, X. W.; Qiao, S. Z. N-doped graphene natively grown on hierarchical ordered porous carbon for enhanced oxygen reduction. *Adv. Mater.* **2013**, *25* (43), 6226−6231.
(10) Bai, R.; Yang, M.; Hu, G.; Xu, L.; Hu, X.; Li, Z.; Wang, S.; Dai, W.; Fan, M. A new nanoporous nitrogen-doped highly-efficient carbonaceous CO_2 sorbent synthesized with inexpensive urea and petroleum coke. *Carbon* **2015**, *81*, 465−473.
(11) Vinu, A.; Ariga, K.; Mori, T.; Nakanishi, T.; Hishita, S.; Golberg, D.; Bando, Y. Preparation and characterization of well-ordered hexagonal mesoporous carbon nitride. *Adv. Mater.* **2005**, *17* (13), 1648−1652.
(12) Jin, X.; Balasubramanian, V. V.; Selvan, S. T.; Sawant, D. P.; Chari, M. A.; Lu, G. Q.; Vinu, A. Highly ordered mesoporous carbon nitride nanoparticles with high nitrogen content: a metal-free basic catalyst. *Angew. Chem., Int. Ed.* **2009**, *48* (42), 7884−7887.
(13) Thomas, A.; Fischer, A.; Goettmann, F.; Antonietti, M.; Muller, J.-O.; Schlogl, R.; Carlsson, J. M. Graphitic carbon nitride materials: variation of structure and morphology and their use as metal-free catalysts. *J. Mater. Chem.* **2008**, *18* (41), 4893−4908.
(14) D'Alessandro, D. M.; Smit, B.; Long, J. R. Carbon dioxide capture: prospects for new materials. *Angew. Chem., Int. Ed.* **2010**, *49* (35), 6058−6082.
(15) Ferey, G.; Serre, C.; Devic, T.; Maurin, G.; Jobic, H.; Llewellyn, P. L.; De Weireld, G.; Vimont, A.; Daturi, M.; Chang, J.-S. Why hybrid porous solids capture greenhouse gases? *Chem. Soc. Rev.* **2011**, *40* (2), 550−562.
(16) Chu, S. Carbon capture and sequestration. *Science* **2009**, *325* (5948), 1599.
(17) Chen, Z.; Deng, S.; Wei, H.; Wang, B.; Huang, J.; Yu, G. Activated carbons and amine-modified materials for carbon dioxide capture — a review. *Front. Environ. Sci. Eng.* **2013**, *7* (3), 326−340.
(18) Hao, G.-P.; Li, W.-C.; Lu, A.-H. Novel porous solids for carbon dioxide capture. *J. Mater. Chem.* **2011**, *21* (18), 6447−6451.
(19) Li, P. Z.; Zhao, Y. Nitrogen-rich porous adsorbents for CO_2 capture and storage. *Chem. - Asian J.* **2013**, *8* (8), 1680−1691.
(20) Sevilla, M.; Valle-Vigón, P.; Fuertes, A. B. N-doped polypyrrole-based porous carbons for CO_2 capture. *Adv. Funct. Mater.* **2011**, *21* (14), 2781−2787.
(21) Chandra, V.; Yu, S. U.; Kim, S. H.; Yoon, Y. S.; Kim, D. Y.; Kwon, A. H.; Meyyappan, M.; Kim, K. S. Highly selective CO_2 capture on N-doped carbon produced by chemical activation of polypyrrole functionalized graphene sheets. *Chem. Commun.* **2012**, *48* (5), 735−737.
(22) Wang, L.; Yang, R. T. Significantly increased CO_2 adsorption performance of nanostructured templated carbon by tuning surface area and nitrogen doping. *J. Phys. Chem. C* **2012**, *116* (1), 1099−1106.
(23) Zhao, Y.; Zhao, L.; Yao, K. X.; Yang, Y.; Zhang, Q.; Han, Y. Novel porous carbon materials with ultrahigh nitrogen contents for selective CO_2 capture. *J. Mater. Chem.* **2012**, *22* (37), 19726−19731.
(24) Zhao, Y.; Liu, X.; Yao, K. X.; Zhao, L.; Han, Y. Superior capture of CO_2 achieved by introducing extra-framework cations into N-doped microporous carbon. *Chem. Mater.* **2012**, *24* (24), 4725−4734.
(25) Zhao, Y.; Yao, K. X.; Teng, B.; Zhang, T.; Han, Y. A perfluorinated covalent triazine-based framework for highly selective and water-tolerant CO_2 capture. *Energy Environ. Sci.* **2013**, *6* (12), 3684−3692.
(26) Zhao, Y.; Liu, X.; Han, Y. Microporous carbonaceous adsorbents for CO_2 separation via selective adsorption. *RSC Adv.* **2015**, *5* (38), 30310−30330.
(27) Zheng, Y.; Liu, J.; Liang, J.; Jaroniec, M.; Qiao, S. Z. Graphitic carbon nitride materials: controllable synthesis and applications in fuel cells and photocatalysis. *Energy Environ. Sci.* **2012**, *5* (5), 6717−6731.
(28) Wu, Z.; Webley, P. A.; Zhao, D. Post-enrichment of nitrogen in soft-templated ordered mesoporous carbon materials for highly efficient phenol removal and CO_2 capture. *J. Mater. Chem.* **2012**, *22* (22), 11379−11389.
(29) Bai, F.; Yang, X.; Li, R.; Huang, B.; Huang, W. Monodisperse hydrophilic polymer microspheres having carboxylic acid groups prepared by distillation precipitation polymerization. *Polymer* **2006**, *47* (16), 5775−5784.
(30) Casco, M. E.; Morelos-Gómez, A.; Vega-Díaz, S. M.; Cruz-Silva, R.; Tristán-López, F.; Muramatsu, H.; Hayashi, T.; Martínez-Escandell, M.; Terrones, M.; Endo, M.; Rodríguez-Reinoso, F.; Silvestre-Albero, J. CO_2 Adsorption on crystalline graphitic nanostructures. *J. CO2 Util.* **2014**, *5* (0), 60−65.
(31) Stein, A.; Wilson, B. E.; Rudisill, S. G. Design and functionality of colloidal-crystal-templated materials-chemical applications of inverse opals. *Chem. Soc. Rev.* **2013**, *42* (7), 2763−2803.
(32) Chatterjee, S.; Nandi, A. K. Tuning of the morphology of a riboflavin-melamine equimolar supramolecular assembly by *in situ*silver nanoparticle formation. *Chem. Commun.* **2011**, *47* (41), 11510−11512.
(33) Barberá, J.; Puig, L.; Romero, P.; Serrano, J. L.; Sierra, T. Propeller-like hydrogen-bonded banana−melamine complexes inducing helical supramolecular organizations. *J. Am. Chem. Soc.* **2006**, *128* (13), 4487−4492.
(34) Kohlmeier, A.; Vogel, L.; Janietz, D. Multiple hydrogen bonded mesomorphic complexes between complementary 1,3,5-triazine and pyrimidine derivatives. *Soft Matter* **2013**, *9* (39), 9476−9486.
(35) Joseph, J.; Jemmis, E. D. Red-, blue-, or no-shift in hydrogen bonds: a unified explanation. *J. Am. Chem. Soc.* **2007**, *129* (15), 4620−4632.
(36) Wang, X.; Maeda, K.; Thomas, A.; Takanabe, K.; Xin, G.; Carlsson, J. M.; Domen, K.; Antonietti, M. A metal-free polymeric photocatalyst for hydrogen production from water under visible light. *Nat. Mater.* **2009**, *8* (1), 76−80.
(37) Dementjev, A. P.; de Graaf, A.; van de Sanden, M. C. M.; Maslakov, K. I.; Naumkin, A. V.; Serov, A. A. X-ray photoelectron spectroscopy reference data for identification of the C_3N_4 phase in carbon−nitrogen films. *Diamond Relat. Mater.* **2000**, *9* (11), 1904−1907.
(38) Li, Q.; Yang, J.; Feng, D.; Wu, Z.; Wu, Q.; Park, S.; Ha, C.; Zhao, D. Facile synthesis of porous carbon nitride spheres with hierarchical three-dimensional mesostructures for CO_2 capture. *Nano Res.* **2010**, *3* (9), 632−642.
(39) Yang, M.; Guo, L.; Hu, G.; Hu, X.; Xu, L.; Chen, J.; Dai, W.; Fan, M. Highly cost-effective nitrogen-doped porous coconut shell-based CO_2 sorbent synthesized by combining ammoxidation with KOH activation. *Environ. Sci. Technol.* **2015**, *49* (11), 7063−7070.
(40) Hao, G. P.; Li, W. C.; Qian, D.; Lu, A. H. Rapid synthesis of nitrogen-doped porous carbon monolith for CO_2 capture. *Adv. Mater.* **2010**, *22* (7), 853−857.
(41) Xia, Y. D.; Mokaya, R.; Walker, G. S.; Zhu, Y. Q. Superior CO_2 adsorption capacity on N-doped, high-surface-area, microporous carbons templated from zeolite. *Adv. Energy Mater.* **2011**, *1* (4), 678−683.
(42) Wang, X. Q.; Liu, C. G.; Neff, D.; Fulvio, P. F.; Mayes, R. T.; Zhamu, A.; Fang, Q.; Chen, G. R.; Meyer, H. M.; Jang, B. Z.; Dai, S. Nitrogen-enriched ordered mesoporous carbons through direct pyrolysis in ammonia with enhanced capacitive performance. *J. Mater. Chem. A* **2013**, *1* (27), 7920−7926.
(43) Cong, H. L.; Zhang, M. R.; Chen, Y. L.; Chen, K.; Hao, Y. J.; Zhao, Y. F.; Feng, L. Highly selective CO_2 capture by nitrogen enriched porous carbons. *Carbon* **2015**, *92*, 297−298.
(44) Wang, J. C.; Senkovska, I.; Oschatz, M.; Lohe, M. R.; Borchardt, L.; Heerwig, A.; Liu, Q.; Kaskel, S. Imine-linked polymer-derived nitrogen-doped microporous carbons with excellent CO_2 capture properties. *ACS Appl. Mater. Interfaces* **2013**, *5* (8), 3160−3167.
(45) Ma, X. Y.; Cao, M. H.; Hu, C. W. Bifunctional HNO_3 catalytic synthesis of N-doped porous carbons for CO_2 capture. *J. Mater. Chem. A* **2013**, *1* (3), 913−918.
(46) Wang, J. C.; Senkovska, I.; Oschatz, M.; Lohe, M. R.; Borchardt, L.; Heerwig, A.; Liu, Q.; Kaskel, S. Highly porous nitrogen-doped polyimine-based carbons with adjustable microstructures for CO_2 capture. *J. Mater. Chem. A* **2013**, *1* (36), 10951−10961.
(47) Myers, A. L.; Prausnitz, J. M. Thermodynamics of mixed-gas adsorption. *AIChE J.* **1965**, *11* (1), 121−127.

DOI: 10.1021/acssuschemeng.5b01230
ACS Sustainable Chem. Eng. 2016, 4, 298−304

(48) Herm, Z. R.; Swisher, J. A.; Smit, B.; Krishna, R.; Long, J. R. Metal-organic frameworks as adsorbents for hydrogen purification and precombustion carbon dioxide capture. *J. Am. Chem. Soc.* **2011**, *133* (15), 5664−5667.
(49) Lu, W.; Yuan, D.; Sculley, J.; Zhao, D.; Krishna, R.; Zhou, H. C. Sulfonate-grafted porous polymer networks for preferential CO_2 adsorption at low pressure. *J. Am. Chem. Soc.* **2011**, *133* (45), 18126−18129.
(50) Mason, J. A.; Sumida, K.; Herm, Z. R.; Krishna, R.; Long, J. R. Evaluating metal-organic frameworks for post-combustion carbon dioxide capture via temperature swing adsorption. *Energy Environ. Sci.* **2011**, *4* (8), 3030−3040.
(51) Qian, D.; Lei, C.; Hao, G.-P.; Li, W.-C.; Lu, A.-H. Synthesis of hierarchical porous carbon monoliths with incorporated metal−organic frameworks for enhancing volumetric based CO_2 capture capability. *ACS Appl. Mater. Interfaces* **2012**, *4* (11), 6125−6132.
(52) Ko, Y. G.; Lee, H. J.; Kim, J. Y.; Choi, U. S. Hierarchically porous aminosilica monolith as a CO_2 adsorbent. *ACS Appl. Mater. Interfaces* **2014**, *6* (15), 12988−12996.

DOI: 10.1021/acssuschemeng.5b01230
ACS Sustainable Chem. Eng. 2016, 4, 298−304